Available online at www.sciencedirect.com
ScienceDirect
Radiation Measurements 43 (2008) 1231–1236
Radiation Measurements
www.elsevier.com/locate/radmeas

Convolution of TLD and SSNTD measurements during the BRADOS-1 experiment onboard ISS (2001)

M. Hajek[a], T. Berger[b,1], N. Vana[a], M. Fugger[a], J.K. Pálfalvi[c,*], J. Szabó[c], I. Eördögh[d], Y.A. Akatov[e], V.V. Arkhangelsky[e], V.A. Shurshakov[e]

[a]*Atomic Institute of the Austrian Universities, Vienna University of Technology, Stadionallee 2, Vienna 1020, Austria*
[b]*German Aerospace Center, Institute of Aerospace Medicine, Linder Höhe, Cologne 51147, Germany*
[c]*Hungarian Academy of Sciences, KFKI Atomic Energy Research Institute, P.O. Box 49, Budapest 1525, Hungary*
[d]*Research Institute for Technical Physics and Material Science, P.O. Box 49, Budapest 1525, Hungary*
[e]*Russian Academy of Sciences, Institute for Biomedical Problems, Koroshevskoye Shosse 76A, Moscow 123007, Russia*

Received 3 October 2006; received in revised form 6 March 2008; accepted 28 April 2008

Abstract

The Russian BRADOS experiment onboard the International Space Station (ISS) was aimed at developing methods in radiation dosimetry and radiobiology to improve the reliability of risk estimates for the radiation environment in low-Earth orbit. Experimental data from thermoluminescence detectors (TLDs) and solid state nuclear track detectors (SSNTDs) gathered during the BRADOS-1 (24 February–31 October 2001) mission are reviewed and convolved to obtain absorbed dose and dose equivalent from primary and secondary cosmic-ray particles. Absorbed dose rates in the ISS Russian Segment (Zvezda) ranged from 208 ± 14 to $275 \pm 14\,\mu Gy\,d^{-1}$. Dose equivalent rates were determined to range from 438 ± 29 to $536 \pm 32\,\mu Sv\,d^{-1}$, indicating a quality factor between 1.95 ± 0.15 and 2.11 ± 0.20. The contribution of densely ionizing particles ($LET \geqslant 10\,keV\,\mu m^{-1}$) to dose equivalent made up between 54% and 64%.
© 2008 Elsevier Ltd. All rights reserved.

Keywords: Space dosimetry; TLD; SSNTD

1. Introduction

The Russian BRADOS research effort onboard the International Space Station (ISS) was realized under the aegis of the Institute for Biomedical Problems (IBMP) of the Russian Academy of Sciences with Austrian and Hungarian participation. The experiment was aimed at developing methods in radiation dosimetry and radiobiology to improve the reliability of risk estimates for the composite radiation environment of solar and galactic origin prevailing in low-Earth orbit (LEO). Cultures of blood cells and salad seeds were exposed in space and under ground-based reference conditions to investigate the potential correlation between operational physical quantities and radiobiological effects. Radiation sensors used onboard the ISS Zvezda Module comprised thermoluminescence detectors (TLDs) from the Atomic Institute of the Austrian Universities (ATI) of the Vienna University of Technology and solid state nuclear track detectors (SSNTDs) from the KFKI-Atomic Energy Research Institute (AERI) of the Hungarian Academy of Sciences. The experiment was initially scheduled to include the following three phases (but continued later): BRADOS-1 (24 February–31 October 2001, 248 days duration), BRADOS-2 (21 March–10 November 2002, 233 days duration) and BRADOS-3 (2 February–28 October 2003, 268 days duration). This paper summarizes and discusses experimental data gathered during BRADOS-1 which have already been published in part by the cooperating laboratories (Berger et al., 2004; Hajek et al., 2006a, b; Pálfalvi et al., 2004, 2005, 2006) and convolves TLD measurements from ATI with SSNTD measurements from AERI.

* Corresponding author. Tel.: +36 1 392 2222 1495; fax: +36 1 395 9162.
E-mail address: palfalvi@sunserv.kfki.hu (J.K. Pálfalvi).
[1] Up to 2003 also Atomic Institute of the Austrian Universities, Vienna University of Technology, Stadionallee 2, Vienna 1020, Austria.

1350-4487/$ - see front matter © 2008 Elsevier Ltd. All rights reserved.
doi:10.1016/j.radmeas.2008.04.094

2. Instruments and methods

The dose determination in space is based on the ICRU 51 (1993) (published also in ICRP 60, 1991; ICRP 74, 1996) quantity "the distribution of the absorbed dose in linear energy transfer" (LET or L) denoted as $D(L)$ in $L+\Delta L$ interval, at a point of interest in a conventionally accepted material (usually in water) and the quality factor, $Q(L)$, defined as a function of the unrestricted LET in liquid water, independent of particle type and analytically expressed in three LET intervals. Then the dose equivalent, $H(L)$ at a point is given as the product of the $D(L)$ and $Q(L)$. To obtain the total absorbed dose (D) and dose equivalent (H) the summation runs over the entire, possible LET range and finally a mean quality factor (Q) can be obtained by dividing H by D.

The acceptance of these quantities for the risk estimation of the astronauts was introduced to the space dosimetry community during the 34th Annual Meeting of the NCRP (Health Physics, 2000) and since the NCRP's recommendations are published (NCRP 2001, 2002, Reports 137 and 142) they are widely used. When passive dosimeters are considered, the dose of particles with LET $\leqslant 10\,\mathrm{keV\,\mu m^{-1}}$ where $Q(L)=1$, can be determined by, for instance, TLD technique, while for higher LET particles usually SSNTDs are used and the absorbed dose is calculated from the so-called differential LET spectrum of the incident particles using the following expression:

$D(L)=\bar{L}\times\Phi(L)$, where $\bar{L}$ is the mean LET in the $L+\Delta L$ interval and the $\Phi(L)$ is the fluence of the incident particles in the same interval (see also Eq. (4)).

2.1. Thermoluminescence detectors

Thermoluminescence dosimetry has become a widely used technique for individual monitoring at terrestrial workplaces. Due to the largely unknown thermoluminescent (TL) efficiency to particles of high charge and energy (HZE) its application to space dosimetry has previously been restricted. This limitation was accounted for by substantial ground-based research in heavy-ion beams, resembling the major aspects of galactic and solar cosmic rays. The relative TL efficiency, $\eta_{k,\gamma}$, is defined as the ratio of TL responses per unit mass and dose from the radiation under study (k) and the ^{60}Co reference radiation (γ)

$$\eta_{k,\gamma}=\frac{R_k/D_k}{R_\gamma/D_\gamma} \tag{1}$$

Herein, R_k and R_γ are the TL signals per unit mass at dose levels of D_k and D_γ, respectively. Relative TL efficiency generally tends to decrease with increasing LET which is likely related to microdosimetric track structure effects (Olko, 2004). Close to the ion's path extremely high doses are deposited locally, the TL signal saturates and the particle energy is less efficiently converted into TL light. However, different particles of the same LET can possess essentially different efficiencies (Berger et al., 2006). Horowitz et al. (2001) attributed this behavior to the complex intermediate mechanisms taking place between radiation absorption and TL emission, but pointed out that a total understanding of the manner in which TL efficiency depends on ionization density was yet to be achieved. For space dosimetry applications, the mean slope of the ^{7}LiF:Mg,Ti (TLD-700) relative TL efficiency, $\bar{\eta}_{k,\gamma}$, as a function of unrestricted LET in water, L, may be approximated by the following three-parameter rational function (Fig. 1) which was derived empirically from experiments at the heavy ion medical accelerator (HIMAC) of the National Institute of Radiological Sciences (NIRS) in Chiba, Japan, for ions with charges from $Z=2$–28 (Hajek et al., 2006a)

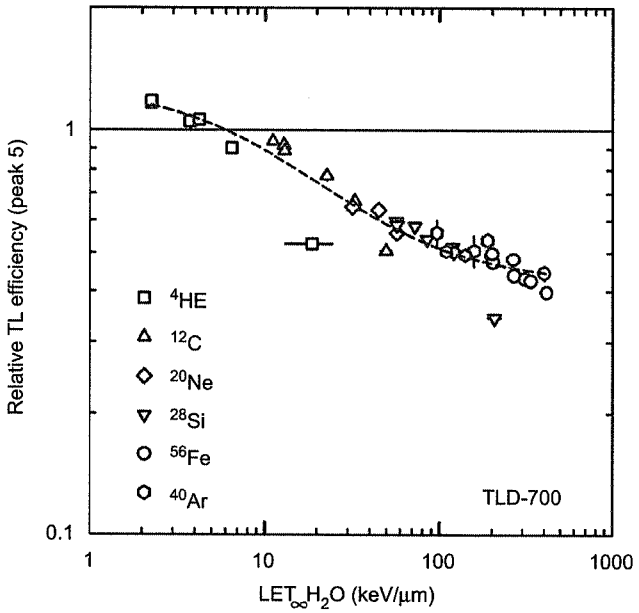

Fig. 1. Relative TL efficiency with respect to ^{60}Co for glow peak 5 in ^{7}LiF:Mg,Ti (TLD-700) for several heavy charged particles.

$$\bar{\eta}_{k,\gamma}(L)=\frac{1+aL}{b+cL} \tag{2}$$

The regression parameters are $a=0.0144\pm0.0043$, $b=0.8021\pm0.0402$ and $c=0.0456\pm0.0092$. TL efficiency values are influenced by the experimental protocol in use, i.e. annealing and readout parameters, method of background subtraction, etc.

The ATI dosemeter stacks accommodated in the BRADOS boxes included commercial TLD-600 (^{6}LiF:Mg,Ti) and TLD-700 (^{7}LiF:Mg,Ti) chips of the dimension $6.4\times6.4\times0.9\,\mathrm{mm^3}$, all obtained from the same batch. Each stack contained four TL chips per type sealed in polystyrene holders, i.e. a total number of eight chips. Preparation included a 400 °C, 1 h anneal and slow cool. Chip-selective pre-and post-flight calibrations in terms of absorbed dose to water were realized at the ^{60}Co γ-theratron of the Clinic for Radiotherapy and Radiobiology, Vienna Medical University. Detector read-out was accomplished in inert nitrogen atmosphere at a heating rate of $5\,^\circ\mathrm{C\,s^{-1}}$.

2.2. Solid state nuclear track detectors

SSNTDs offer several advantages to gather information on the type and energy of particle radiations. A simple

Table 1
List of particles used for the SSNTD calibration

Particle—Provider	Energy (GeV)	$LET_{\infty}H_2O$ (keV μm^{-1})
^{12}C, bare—NIRS	1.22	25.6
^{12}C + 16.6 mm PMMA—NIRS	0.59	45.1
^{40}Ar, bare—NIRS	18.9	94.6
^{40}Ar + 75.7 mm PMMA—NIRS	9.1	139
^{40}Ar, bare—NIRS	18.4	95.7
^{40}Ar + 40 mm PMMA—NIRS	13.1	113
^{56}Fe + 2.6 mm PMMA—NIRS	5.1	524
^{56}Fe, bare—NSRL/BNL	48.5	152
^{56}Fe 37 mm Al—NSRL/BNL	36.1	166
^{84}Kr, bare—NIRS	24.5	465
^{84}Kr + 16.6 mm PMMA—NIRS	14.0	655
Proton—Van de Graaf, AERI	1.0 MeV	240
^{210}Po α—AERI	4.65 MeV	96.2

The energy and LET values were calculated from the nominal values by the SRIM2003 code for the surface of the detector sheet taking into account the filtration and detector cover.

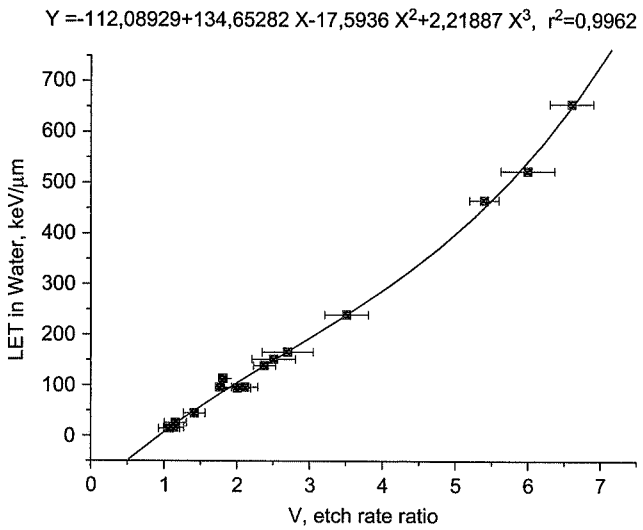

Fig. 2. Calibration curve for the TASTRAK PADC detectors showing the track etch rate ratio, V, as a function of unrestricted LET in water, L.

stack of track detectors permits determining the high-LET ($\geqslant 10\,\mathrm{keV\,\mu m^{-1}}$) radiation dose received by ISS crews. The radiation field inside the ISS is composed of primary cosmic-ray particles penetrating the wall of the ISS and secondaries, mainly neutrons induced by primaries in the wall and other structural materials surrounding the detectors. From the analysis of the tracks induced by these particles LET spectra, absorbed dose and dose equivalent can be computed. For that purpose, an experimental calibration function is required assuming a well-defined correlation between measurable track parameters and the track etch rate ratio, V, and between V and L (Durrani and Bull, 1987). Several calibrations were performed by exposing detectors to perpendicularly incident charged particles available from the NIRS–HIMAC and the NASA Space Radiation Laboratory (NSRL)–Brookhaven National Laboratory (BNL) high-energy accelerators in the framework of the ICCHIBAN project (Yasuda et al., 2006) as well as from isotopic sources (see Table 1). The calibration function obtained for the employed polyallyl diglycol carbonate (PADC) detectors (TATSTRAK, Bristol) is presented in Fig. 2.

It was found that a polynomial fit can well describe the relationship between track etch rate ratio, V, and unrestricted LET in water, L. The presented function is strictly valid for etching off an 8-μm-thick layer from the TASTRAK PADC detector (1 mm) in 6 N NaOH at 70 °C in 6 h. It must be noted that there is a slight variation in the track registration ability of this detector material even within the same production batch. This implicates an uncertainty in the lowest determinable LET threshold between 10 and 15 keV μm^{-1} and, consequently, in the particle fluence below 15 keV μm^{-1}. However, this does not hamper efficiency correction of the TLDs, since relative efficiency is close to unity in this low-LET region (Fig. 1). The number of detected particles, N, in a given LET interval is further corrected below $\sim 50\,\mathrm{keV\,\mu m^{-1}}$ to get the effective particle number, $N_{\mathrm{eff}} = N \cdot f_c$, considering a dip angle dependence according to a correction method proposed by Tawara et al. (2002) and described by Eq. (3) where the f_c is the correction factor and V is the averaged track etch ratio within the given LET interval as calculated from the track parameter measurements. $\eta(L)$ is the weighted dip angle correction factor in the same LET interval obtained from experiments:

$$f_c = \eta(L) \cdot \frac{V^2}{V^2 - 1} \tag{3}$$

Determination of the dose equivalent, H, is based on the following equation using the quality factors recommended by ICRP (1991)

$$H = \frac{1}{\rho} \cdot 1.602 \cdot 10^{-6} \cdot \sum_i \Phi_i(L_i)\bar{L}_i Q_i(L_i)\Delta L_i \tag{4}$$

where ρ is the tissue density (1 g cm^{-3} for water, in our case), $\Phi_i(L_i)$ is the corrected total group fluence (N_{eff}/A, cm^{-2}) measured for the entire exposure time and in the interval ΔL_i, $\bar{L}_i$ is the mean LET and $Q_i(L_i)$ is the quality factor in that interval. The factor $1.602 \cdot 10^{-6}$ harmonizes the units to obtain the dose equivalent in mSv. Without applying the quality factor, the absorbed dose for $\mathrm{LET} \geqslant 10\,\mathrm{keV\,\mu m^{-1}}$, $D_{\mathrm{SSNTD} \geqslant 10}$, can be obtained.

Owing to the limited volume available in the BRADOS boxes, the stacks were composed of three PADC sheets (TASTRAK, Bristol), each 20 × 50 × 1 mm^3 in size. The stack was wrapped in a thin (30 μm) aluminum foil and sealed hermetically in a polyethylene bag of 40 μm thickness. The chemical etching was made in 6 N NaOH at 70 °C for 6 h. All the detectors were pre-etched before sending for exposure to eliminate and register possible background tracks. Sheets with uniform thickness and low background were selected. After pre-etching, one corner of each sheet was exposed to a collimated beam of α particles emitted by a home made ^{210}Po source to obtain a reference track etch rate of a known LET particle. The bulk etch rate, $V_B = 1.34\,\mu\mathrm{m\,h^{-1}}$, was studied in two steps: by weight measurements and following the diameter growth of circular,

high LET tracks. When evaluating the detectors exposed on the ISS no latent track fading was taken into consideration.

Evaluation of the etched detectors is based on the VIRGINIA image analyzer (Pálfalvi et al., 1997). It consists of a high-resolution microscope coupled to a CCD camera. The video signal is captured and fed into a high-speed electronic device for analogue processing (image quality enhancement, background compensation etc.) and digitization. The "teachable" pattern recognizing software maps the tracks and stores many measured parameters including position, grey level distribution and geometrical data. Using a set of patterns collected from calibrations and related to different kinds of tracks, the classification of tracks is done automatically. The home made analysis software provides the LET spectrum, the absorbed dose and dose equivalent.

2.3. Convolution of TLD and SSNTD measurements

The highly complex nature and broad LET range of the radiation field encountered onboard space vehicles (Benton and Benton, 2001) represents one of the outmost challenges in instrument design. TLDs detect the low-LET component ($< 10\,\mathrm{keV\,\mu m^{-1}}$) with a relative efficiency of ~ 1, but particles with charges of $Z > 2$ are registered with significantly lower efficiency. Dose contributions of these ions are thus underestimated in the integral TL signal. Conversely, SSNTDs are insensitive to particles with LET $< 10\,\mathrm{keV\,\mu m^{-1}}$. Convolution of TLD and SSNTD measurements compensates the shortcomings of both detectors by separating total dose and dose equivalent into low- and high-LET portions, similar to a method described by Benton et al. (2002). The reduced high-LET response of TLD-700 is characterized by Eq. (2) and used to correct dose from particles of LET $\geqslant 10\,\mathrm{keV\,\mu m^{-1}}$. The low-LET component, D_{L}, for which the quality factor $Q = 1$, is

$$D_{\mathrm{L}} = D_{\mathrm{TLD}} - \sum_i \bar{\eta}_{\mathrm{k},\gamma}(L_i) D_{\mathrm{SSNTD}\geqslant 10}(L_i)\Delta L_i \quad (5)$$

The folding integral spans over the LET range 10–300 keV $\mu\mathrm{m}^{-1}$ and is approximated by a sum over discrete LET intervals of width $\Delta L = 5\,\mathrm{keV\,\mu m^{-1}}$. D_{TLD} is the absorbed dose determined from the integral TL signal. $D_{\mathrm{SSNTD}\geqslant 10}$ and, in the following, $H_{\mathrm{SSNTD}\geqslant 10}$ are assessed directly from the LET spectrum $\geqslant 10\,\mathrm{keV\,\mu m^{-1}}$ measured in the PADC sheets. In determining dose equivalent, the ICRP 60 definition of quality factor was used (ICRP, 1991). The total absorbed dose, D_{total}, is given by

$$D_{\mathrm{total}} = D_{\mathrm{L}} + D_{\mathrm{SSNTD}\geqslant 10} \quad (6)$$

The total dose equivalent, H_{total}, is derived from

$$H_{\mathrm{total}} = D_{\mathrm{L}} + H_{\mathrm{SSNTD}\geqslant 10} \quad (7)$$

The average quality factor, $\bar{Q}$, is then

$$\bar{Q} = \frac{H_{\mathrm{total}}}{D_{\mathrm{total}}} \quad (8)$$

Mean absorbed dose and dose equivalent rates were calculated by dividing absorbed dose and dose equivalent, respectively, by the exposure duration.

3. Results and discussion

3.1. TLD-700 absorbed dose measurements of low LET radiation

Absorbed dose rates were measured with TLD-700 during the BRADOS-1 experiments and are reported in Table 2. TL efficiency correction has not been applied. For each panel, the average of four detector chips was calculated. Statistical uncertainties correspond to a 95% confidence level (2σ).

The dose rates measured during the BRADOS-1 experiment ranged between $198 \pm 4\,\mu\mathrm{Sv\,d^{-1}}$ in panel no. 318 (core block ceiling by central axis) and $265 \pm 14\,\mu\mathrm{Sv\,d^{-1}}$ in panel no. 110 (core block by central axis, floor). For comparison also the dose rates measured during the BRADOS-2 mission in 2002 are given, which were generally lower (Hajek et al., 2006b). Both experiments were carried out at similar solar activity conditions around the maximum of the 23rd solar cycle. However, in 2001 the ISS orbit was rather unstable with a considerable number of altitude changes. In 2002, the Station has been stabilized at a lower orbit which explains the observed differences in dose rate. For the BRADOS-2 experiment, the lowest dose rate of

Table 2
Absorbed dose rates, $\dot{D}_{\mathrm{TLD}}$, measured with TLD-700 during the BRADOS-1 experiment (24 February–31 October 2001)

Box no.	Panel no.	Description	$\dot{D}_{\mathrm{TLD}}$ ($\mu\mathrm{Gy\,d^{-1}}$)
A14	457	Core block starboard side, toilet	200 ± 14
A15	318	Core block by central axis, ceiling	198 ± 4
A16	110	Core block by central axis, floor	265 ± 14

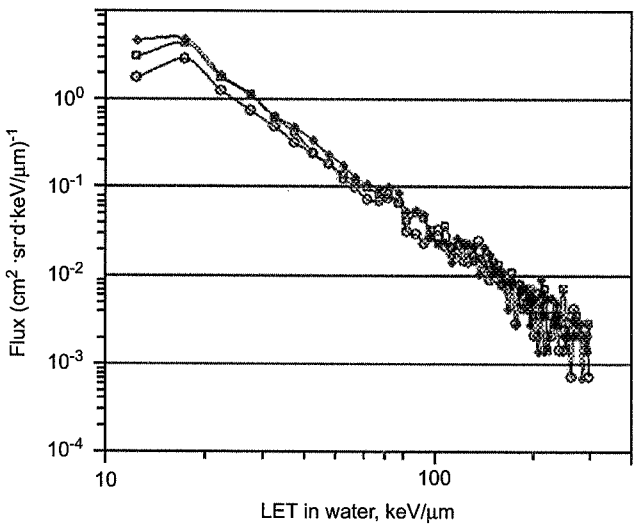

Fig. 3. Differential LET spectra obtained by SSNTD measurements (BRADOS-1) in boxes A14 (○), A15 (◆) and A16 (□).

Table 3
Absorbed dose rates from low LET ($< 10\,\mathrm{keV\,\mu m^{-1}}$), $\dot{D}_L$, high LET ($\geqslant 10\,\mathrm{keV\,\mu m^{-1}}$), $\dot{D}_{SSNTD\geqslant 10}$, and total absorbed dose rate, $\dot{D}_{total}$, determined by convolving TLD with SSNTD data gathered during the BRADOS-1 experiment (24 February–31 October 2001)

Box no.	Panel no.	$\dot{D}_L$ ($\mu Gy\,d^{-1}$)	$\dot{D}_{SSNTD\geqslant 10}$ ($\mu Gy\,d^{-1}$)	$\dot{D}_{total}$ ($\mu Gy\,d^{-1}$)
A14	457	185 ± 14	23 ± 2	208 ± 14
A15	318	176 ± 6	33 ± 3	209 ± 7
A16	110	246 ± 14	29 ± 3	275 ± 14

Table 4
Dose equivalent rate, $\dot{H}_{SSNTD\geqslant 10}$, and mean quality factor, $\bar{Q}_{SSNTD\geqslant 10}$, from high LET ($\geqslant 10\,\mathrm{keV\,\mu m^{-1}}$), total dose equivalent rate, $\dot{H}_{total}$, and mean quality factor, $\bar{Q}_{total}$, determined by convolving TLD with SSNTD data gathered during the BRADOS-1 experiment (24 February–31 October 2001)

Box no.	Panel no.	$\dot{H}_{SSNTD\geqslant 10}$ ($\mu Sv\,d^{-1}$)	$\bar{Q}_{SSNTD\geqslant 10}$	$\dot{H}_{total}$ ($\mu Sv\,d^{-1}$)	$\bar{Q}_{total}$
A14	457	253 ± 25	11.0 ± 1.5	438 ± 29	2.11 ± 0.20
A15	318	311 ± 31	9.42 ± 1.3	487 ± 32	2.33 ± 0.17
A16	110	290 ± 29	10.0 ± 1.4	536 ± 32	1.95 ± 0.15

The quality factor for the low LET part was $Q_L = 1$.

$180 \pm 10\,\mu Sv\,d^{-1}$ was measured in panel no. 327 (core block ceiling, atop R-16 radiometer), compared to the highest dose rate of $223 \pm 8\,\mu Sv\,d^{-1}$ in panel no. 110 (core block floor by central axis). Relatively low dose rates were found also in the starboard-side toilet (panels no. 455 and 457) which is attributed to the shielding effect of the surrounding water pipes.

3.2. LET spectra, absorbed dose and dose equivalent of high LET radiation

The dimensions of the SSNTD stack made it impossible to investigate accurately the long-range HZE particles, which penetrated the entire stack, their number was relatively small. They were thus not considered in this study. The LET spectra were determined from the analysis of the tracks on the top surface of the stack.

LET spectra for the BRADOS-1 experiment are summarized in Fig. 3. Statistical error bars (based on Poisson distribution) are not given on the plots to avoid chaotic picture and they would not characterize the overall uncertainty. The uncertainty of the flux in the LET range below $15\,\mathrm{keV\,\mu m^{-1}}$, close to the detection threshold is estimated to be 50%, between 15 and $25\,\mathrm{keV\,\mu m^{-1}}$ it reaches 30% mainly due to the uncertainty in track parameter measurements of small tracks. With increasing LET, the uncertainty decreases down and reaches 10% at $\sim 150\,\mathrm{keV\,\mu m^{-1}}$ and increasing again up to 30% for higher LET at $\sim 200\,\mathrm{keV\,\mu m^{-1}}$ or even higher because of the decreasing number of tracks. The number of tracks identified having a LET $> 300\,\mathrm{keV\,\mu m^{-1}}$ was negligible; therefore the spectra end here but the particles were considered for the dose calculations.

The calculated charged particle absorbed dose rate and dose equivalent rate values for LET $\geqslant 10\,\mathrm{keV\,\mu m^{-1}}$ are given in Tables 3 and 4. The absorbed dose uncertainty (1σ) was obtained as the weighted average error for the entire LET interval and found to be $< 18\%$, including the uncertainty of the calibration function ($\sim 8\%$) and the uncertainty of the LET dependent detection efficiency ($\sim 8\%$).

SSNTD stacks were used during the BRADOS-3 experiments, as well. For comparison some (unpublished) result are given here. The absorbed dose rate varied from place to place between 11 and $19\,\mu Gy\,d^{-1}$, meanwhile the dose equivalent rate ranged from 182 to $251\,\mu Sv\,d^{-1}$. These values are somewhat lower than found during the BRADOS-1 experiments, similarly to the results of the TLD measurements. The general trend of the decreasing dose rate can be attributed partly to the change in the orbital parameters. Though, the panel numbers were the same during both exposures, it is not known whether the positions of the boxes were the same on the panels. The shielding thickness in front of the BRADOS boxes is not exactly known. It varies from ~ 6 up to $17\,g\,cm^{-2}$. Also, the shielding might be changed during the time by placing or removing objects.

3.3. Convolved TLD/SSNTD dose determination

Total absorbed dose and dose equivalent rates were calculated from convolution of TLD with SSNTD data according to the method described above. Results are presented in Tables 3 and 4 for BRADOS-1 detector boxes which contained both TLDs and SSNTDs, i.e. A14 (panel no. 457), A15 (panel no. 318) and A16 (panel no. 110). Statistical uncertainties correspond to a 95% confidence level (2σ) and have been determined according to the principles of error propagation. For the convolution procedure, LET spectra $\geqslant 10\,\mathrm{keV\,\mu m^{-1}}$ were used.

4. Conclusions

The evaluation method of the SSNTDs based on the calibrations at high energy particle accelerators allow to obtain the particle LET spectrum (LET $\geqslant 10\,\mathrm{keV\,\mu m^{-1}}$) which makes it possible to correct the absorbed dose measured by TLDs for dose contributions from high-LET ions which are underestimated in the integral TL signal. The corrected TLD dose value can be summed up with the absorbed dose derived from the LET spectrum as shown in Table 2. Here, it can be seen that

the contribution of the high-LET charged particles to the total absorbed dose is approximately 10%. However, their contribution to the dose equivalent is equally important (see Table 3) because of the higher quality factor of the order of 10.

Depending on the shielding conditions, the resulting total dose equivalent rates agree well with the average dose equivalent rate of 413 $\mu Sv\,d^{-1}$ recorded during the Dosimetric Mapping (DOSMAP) experiment inside the US Destiny Laboratory Module of the ISS employing as well a combination of TLD and SSNTD techniques (Reitz et al., 2005). The dose equivalent rates measured by the DOSTEL telescope (535 $\mu Sv\,d^{-1}$) and the NASA tissue-equivalent proportional counter (TEPC, 467 $\mu Sv\,d^{-1}$) for the US Module are somewhat higher which can be explained by the response characteristics of these instruments.

In conclusion, it can be stated, that the two passive dosimetry systems, TLD and SSNTD, complement each other since they are able to measure the absorbed dose of the low- and high-LET radiation components, respectively, and thus provide the possibility to obtain the total absorbed dose and the dose equivalent characterizing the radiation field on the ISS and the radiation hazard of the astronauts.

Acknowledgments

The BRADOS project has been supported in part by the Austrian Federal Ministry of Transport, Innovation and Technology (Contract no. 140.596/3-V/B/9b/2000) and the Hungarian Space Office (Project no. TP-174). The assistance of Yukio Uchihori, Nakahiro Yasuda and Hisashi Kitamura during the TL—efficiency experiments at NIRS–HIMAC (Project no. 16P-169) is highly acknowledged. Further on we want to thank the operation staff at HIMAC as well as our colleagues from NIRS for giving us the opportunity to participate in the ICCHIBAN intercomparison project.

References

Benton, E.R., Benton, E.V., 2001. Space radiation dosimetry in low-Earth orbit and beyond. Nucl. Instrum. Methods B 184, 255–294.

Benton, E.R., Benton, E.V., Frank, A.L., 2002. Passive dosimetry aboard the Mir Orbital Station: internal measurements. Radiat. Meas. 35, 439–455.

Berger, T., Hajek, M., Summerer, L., Vana, N., Akatov, Y., Shurshakov, V., Arkhangelsky, V., 2004. Austrian dose measurements onboard space station Mir and the International Space Station—overview and comparison. Adv. Space Res. 34, 1414–1419.

Berger, T., Hajek, M., Summerer, L., Fugger, M., Vana, N., 2006. The efficiency of various thermoluminescence dosemeter types to heavy ions. Radiat. Protect. Dosim. 120, 365–368.

Durrani, S.A., Bull, R.K., 1987. Solid State Nuclear Track Detection: Principles, Methods, and Applications. Pergamon Press, Oxford. 284pp.

Hajek, M., Berger, T., Fugger, M., Fuerstner, M., Vana, N., Akatov, Y., Shurshakov, V., Arkhangelsky, V., 2006a. BRADOS—dose determination in the Russian Segment of the International Space Station. Adv. Space Res. 37, 1664–1667.

Hajek, M., Berger, T., Fugger, M., Fürstner, M., Vana, N., Akatov, Y., Shurshakov, V., Arkhangelsky, V., 2006b. Dose distribution in the Russian Segment of the International Space Station. Radiat. Prot. Dosim. 120, 446–449.

Health Physics, 2000. 34th Annual Meeting of the NCRP: Cosmic Radiation Exposure of Airline Crews, Passengers and Astronauts, vol. 79(5).

Horowitz, Y.S., Avila, O., Rodríguez-Villafuerte, M., 2001. Theory of heavy charged particle response efficiency and supralinearity in TL materials. Nucl. Instrum. Methods B 184, 85–112.

ICRP, 1991. International Commission on Radiological Protection, Publication 60: 1990 Recommendations of the International Commission on Radiological Protection. Elsevier Science, New York.

ICRP, 1996. International Commission on Radiological Protection, Publication 74: Conversion Coefficients for Use in Radiological Protection against External Radiation. Elsevier Science, New York.

ICRU, 1993. International Commission on Radiation Units and Measurements, Report 51: Quantities and Units for Ionizing Radiation. Bethesda, Maryland.

NCRP, 2001. National Council on Radiation Protection and Measurements, Report 137: Fluence-based and Microdosimetric Event-based Methods for Radiation Protection in Space. Bethesda, Maryland.

NCRP, 2002. National Council on Radiation Protection and Measurements, Report 142: Operational Radiation Safety Program for Astronauts in Low Earth Orbit: A Basic Framework. Bethesda, Maryland.

Olko, P., 2004. Microdosimetric modelling of the relative efficiency of thermoluminescent materials. Radiat. Meas. 38, 781–786.

Pálfalvi, J.K., Eördögh, I., Szász, K., Sajó-Bohus, L., 1997. A new generation image analyser for evaluating SSNTDs. Radiat. Meas. 28, 849–852.

Pálfalvi, J.K., Akatov, Y., Szabó, J., Sajó-Bohus, L., Eördögh, I., 2004. Evaluation of solid state nuclear track detector stacks exposed on the International Space Station. Radiat. Prot. Dosim. 110, 393–397.

Pálfalvi, J.K., Szabó, J., Akatov, Y., Sajó-Bohus, L., Eördögh, I., 2005. Cosmic ray studies on the ISS using SSNTD, BRADOS projects, 2001–2003. Radiat. Meas. 40, 428–432.

Pálfalvi, J.K., Akatov, Y., Szabó, J., Sajó-Bohus, L., Eördögh, I., 2006. Detection of primary and secondary cosmic ray particles aboard the ISS using SSNTD stacks. Radiat. Prot. Dosim. 120, 427–432.

Reitz, G., Beaujean, R., Benton, E., Burmeister, S., Dachev, TS., Deme, S., Luszik-Bhadra, M., Olko, P., 2005. Space radiation measurements on-board ISS—the DOSMAP experiment. Radiat. Prot. Dosim. 116, 374–379.

Tawara, H., Doke, T., Hayashi, T., Kikuchi, J., Kyan, A., Nagaoka, S., Nakano, T., Takahashi, S., Terasawa, K., Yoshihira, E., 2002. LET distributions from CR-39 plates on Space Shuttles missions STS-84 and STS-91 and a comparison of the results of the CR-39 plates with those of RRMD-II and RRMD-III telescopes. Radiat. Meas. 35, 119–126.

Yasuda, N., Uchihori, Y., Benton, E.R., Kitamura, H., Fujitaka, K., 2006. The intercomparison of cosmic rays with heavy ion beams at NIRS ICCHIBAN project. Radiat. Prot. Dosim. 120, 414–420.